9th Asia-Pacific Conference on Wind Engineering
Auckland, New Zealand
3-7 December 2017

Numerical Evaluation of Nonlinear Coupled Galloping of A Slender Tower

Liang Wu and Delong Zuo

[1]Department of Civil, Environmental and Construction Engineering, Texas Tech University, Lubbock, TX 79409, USA

Abstract

An analytical model based on quasi-steady assumption of wind loading is formulated to assess the galloping of slender towers that are nonlinearly coupled in two directions about the principal axes. To illustrate the effectiveness of this model, it is used to evaluate the responses of a full-scale slender tower subjected to excitation from winds simulated using the spectral representation method. Some of the numerical results are compared with field observations of wind-induced galloping oscillations of this tower. The characteristics of the oscillations, including the root mean square (RMS) amplitudes and the kurtosis, and the dependence of these characteristics on the mean wind speed and the turbulence are presented.

Introduction

Slender towers are commonly used as supports for objects such as luminaires and antenna of various kinds. This type of structure can be susceptible to wind excitation because they are flexible and often possess low levels of damping. In some cases, wind-induced oscillation has become excessive and resulted in failures of the towers [e.g., 1, 2]. While a number of excitation mechanisms, including galloping, vortex shedding and buffeting, can all lead to significant vibrations of the towers, galloping has often been identified as the most problematic and responsible for the failures due to the large amplitudes that this type of vibration can reach [1, 3]. This is primarily because the shapes of the cross-sections of some towers (such as square or rectangular cross-sections) lead to the generation of self-excited forces in the form of aerodynamic damping when wind approaches from certain directions. In addition, towers with cross-sections that do not tend to gallop, such as circular cross-sections, can also be susceptible to galloping in certain weather conditions, as their small cross-sections can be significantly changed by external matters such as snow or ice and become galloping prone.

One type of galloping oscillation of slender towers is of particular interest. It differs from the classical across-wind galloping in that it involves coupling between translations in directions about the two principal axes of the towers. Due to the coupling, methods for the assessment of the galloping onset condition, including those based on the Den Hartog criterion [4], which only considers the mean wind speed, and the models that also consider the turbulence [5], and models for predicting the amplitude of the across-wind vibration, such as those that represent the self-excited forces by polynomials (e.g., [6, 7]) or Fourier series [8] of the oscillation velocity, are no longer applicable. A number of studies have proposed models for coupled galloping of slender structures. Jones first formulated an eigenvalue problem that can be solved to yield a criterion for the onset of galloping involving coupling between the along-wind and across-wind degrees of freedom [9]. However, this formulation is restrictive because it requires the interacting modes to be of an identical frequency and the wind to be along one of the principal axes. A number of subsequent studies attempted to address these limitations in Jones' formulation. Liang [10] relaxed the restriction on the frequencies of the modes that participate in the coupling as well as that on the wind direction. However, this study resulted in an erroneous conclusion that coupled translational galloping occurs only when the frequencies of the two modes about the principal axes are the same because the solution assumed the vibration in these two modes to be in phase. The problem of coupled galloping was also addressed as part of an effort to model a perceived type of wind-induced dry stay cable vibration (e.g., [11, 12]). Although these studies included the effect of the Reynolds number on the wind loading of circular cylinders, the general formulation of the equations of motion and the approach used to obtain the solutions in terms of the onset conditions of coupled galloping are also applicable to the cases in which the Reynolds number is not relevant. A more recent study provided a comprehensive treatment of the galloping problem and highlighted the effects of factors such as the frequency difference of the participating modes on the onset and the characteristics of coupled translational galloping [13]. However, due to linearization of the problem, the results of this study are valid only for galloping oscillations of small amplitudes. In another recent study, the equation of coupled galloping of a slender structure in boundary layer flow was derived and used to assess the coupled galloping of a full-scale tower [3]. This study, however, also only focused on the onset of the galloping oscillation.

In addition to the studies of the instability boundary of coupled galloping, several investigations have also been used to study the response of the structure post galloping onset. Li. et al. formulated the nonlinear equations of coupled galloping of slender structures in turbulent flow [14]. However, in an illustrative application, this study unrealistically assumed the turbulence to be fully correlated along the height of the structure. In an effort to advance the understanding of dry cable galloping, Raeesi et al. derived for the nonlinear equations of galloping motion of an inclined circular cylinder and used these equations as a basis to numerically assess the galloping response of the cylinder subjected to turbulent flows [15]. Although the effects of the Reynolds number are included in the equations, a reduced version of this model can be readily applied to the cases when Reynolds number effect is trivial. These equations, however, are only for a two degree of freedom cylinder sections in uniform flow and cannot be used to model the galloping oscillation of a full-scale elastic towers in sheared boundary layer flow.

This paper presents the formulation of the nonlinear equations of coupled translational galloping of an elastic slender structure in state-space form. These equations are used as a basis to numerically assess the galloping of a full-scale tower in simulated boundary layer flow. The effects of the turbulence intensity of the flow and the structural damping of the tower on the major characteristics of the vibration are investigated.

Analytical Formulation

Figure 1 schematically depicts the wind components, the forces acting on a section of unit length of a slender structure and the

translations of the section about its principal axes. In this graph, $\bar{U}$ is the mean along-wind speed, u and v are the along-wind and across-wind components of the turbulence, $\bar{r}_x$ and $\bar{r}_y$ are the mean displacements of the section in the directions of the principal axes, r_x and r_y are the dynamic displacements, D and L are the drag and lift forces, respectively, $\bar{\alpha}$ is the angle of incidence of the mean wind component defined relative to the principle axis x, $\Delta\alpha$ is the increment of the angle of incidence of the total horizontal wind speed relative to the cross-section, the magnitude of which is U_{rel}, and α is the total angle of incidence of the relative wind speed.

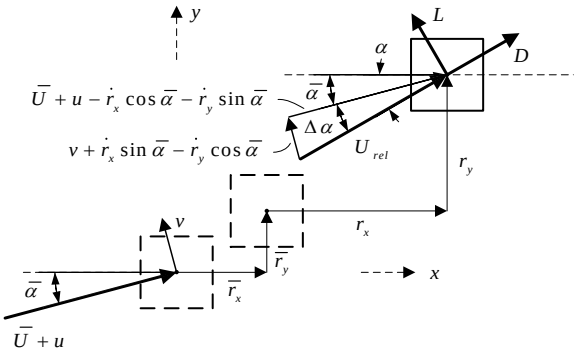

Figure 1. Instantaneous wind and force components and the resultant translations of a structural section

Using the quasi-steady assumption, the drag and lift forces acting on the section of unit length can be expressed as

$$\begin{bmatrix} D & L \end{bmatrix}^T = \frac{1}{2}\rho U_{rel}^2 B\begin{bmatrix} C_D(\alpha) & C_L(\alpha) \end{bmatrix}^T \tag{1}$$

in which $C_D(\alpha)$ and $C_L(\alpha)$ are the drag and lift force coefficients measured at the angle of incidence α in wind tunnel tests of static models of the section. Since $u \ll \bar{U}$ and $v \ll \bar{U}$, $\Delta\alpha$ and U_{rel}^2 can be expressed as

$$\Delta\alpha = \arctan\left(\frac{v+\dot{r}_x\sin\bar{\alpha}-\dot{r}_y\cos\bar{\alpha}}{\bar{U}+u-\dot{r}_x\cos\bar{\alpha}-\dot{r}_y\sin\bar{\alpha}}\right) \tag{2}$$

$$\begin{aligned} U_{rel}^2 \approx{}& \bar{U}^2 + 2u\bar{U} - 2\left[(\bar{U}+u)\cos\bar{\alpha} - v\sin\bar{\alpha}\right]\dot{r}_x \\ & -2\left[(\bar{U}+u)\sin\bar{\alpha} + v\cos\bar{\alpha}\right]\dot{r}_y + \dot{r}_x^2 + \dot{r}_y^2 \end{aligned} \tag{3}$$

The force components in the directions of the principal axes are

$$\mathbf{f} = \begin{bmatrix} f_x \\ f_y \end{bmatrix} = \begin{bmatrix} \cos\alpha & -\sin\alpha \\ \sin\alpha & \cos\alpha \end{bmatrix}\begin{bmatrix} D \\ L \end{bmatrix} \tag{4}$$

For a section of unit length, the equation of motion is.

$$\mathbf{m}\ddot{\mathbf{r}} + \mathbf{c}\dot{\mathbf{r}} + \mathbf{m}\boldsymbol{\Omega}^2\mathbf{r} = \mathbf{f} \tag{5}$$

where

$$\mathbf{r} = \begin{bmatrix} r_x \\ r_y \end{bmatrix};\ \mathbf{m} = \begin{bmatrix} m(z) & 0 \\ 0 & m(z) \end{bmatrix};\ \mathbf{c} = \begin{bmatrix} c_{xx} & 0 \\ 0 & c_{yy} \end{bmatrix};\ \boldsymbol{\Omega}^2 = \begin{bmatrix} \omega_x^2 & 0 \\ 0 & \omega_y^2 \end{bmatrix} \tag{6}$$

In which $m(z)$ is the mass per unit length of the structure at height z, c_{xx} and c_{yy} are the damping coefficients about the principal axes, and ω_x and ω_y are the natural frequencies of the structure in these directions. Assuming that the vibration of a slender tower is dominated by one mode each about the principle axes, the translational displacements of a slender tower at a height of z above ground can be expressed as

$$\mathbf{r} = \boldsymbol{\Phi}(z)\mathbf{q}(t) \tag{7}$$

in which

$$\boldsymbol{\Phi}(z) = \begin{bmatrix} \phi_x(z) & 0 \\ 0 & \phi_y(z) \end{bmatrix};\ \boldsymbol{q}(t) = \begin{bmatrix} q_x(t) \\ q_y(t) \end{bmatrix} \tag{8}$$

are the modal matrix and the generalized coordinate vector, respectively. With equation (7), the generalized equations of motion of a slender tower of height h is

$$\mathbf{M}\ddot{\mathbf{q}} + \mathbf{C}\dot{\mathbf{q}} + \mathbf{M}\boldsymbol{\Omega}^2\mathbf{q} = \mathbf{F} \tag{9}$$

where

$$\mathbf{M} = \begin{bmatrix} M_x & 0 \\ 0 & M_y \end{bmatrix};\ \mathbf{C} = \begin{bmatrix} C_{xx} & 0 \\ 0 & C_{yy} \end{bmatrix};\ \mathbf{F} = \begin{bmatrix} F_x \\ F_y \end{bmatrix} \tag{10}$$

are the generalized mass, damping matrices and the generalized force vector. The elements of these matrices and vector are

$$M_x = \int_0^h m(z)\phi_x^2(z)dz;\ M_y = \int_0^h m(z)\phi_y^2(z)dz \tag{11}$$

$$C_{xx} = 2M_x\omega_x\zeta_x;\ C_{yy} = 2M_y\omega_y\zeta_y \tag{12}$$

$$F_x = \int_0^h f_x\phi_x(z)dz;\ F_y = \int_0^h f_y\phi_y(z)dz \tag{13}$$

In equation (12), ζ_x and ζ_y are the damping to critical ratios of the modes of interest.

Equation (9) can be alternatively written in state-space form as

$$\dot{\boldsymbol{\eta}} = \mathbf{A}\boldsymbol{\eta} + \mathbf{B}\mathbf{F} \tag{14}$$

in which

$$\boldsymbol{\eta} = \begin{bmatrix} q_x & q_y & \dot{q}_x & \dot{q}_y \end{bmatrix}^T;\ \mathbf{F_b} = \begin{bmatrix} 0 & 0 & F_x & F_y \end{bmatrix}^T \tag{15}$$

$$\mathbf{A} = \begin{bmatrix} 0 & 0 & 1 & 0 \\ 0 & 0 & 0 & 1 \\ -\omega_x^2 & 0 & -2\omega_x\zeta_x & 0 \\ 0 & -\omega_y^2 & 0 & -2\omega_y\zeta_y \end{bmatrix};\ \mathbf{B} = \begin{bmatrix} 0 & 0 & 0 & 0 \\ 0 & 0 & 0 & 0 \\ 0 & 0 & 1/M_x & 0 \\ 0 & 0 & 0 & 1/M_y \end{bmatrix} \tag{16}$$

Since both U_{rel}^2 and $\alpha = \bar{\alpha} + \Delta\alpha$ are nonlinear functions of the velocities of the translation, $\dot{r}_x$ and $\dot{r}_y$, equation (14) is a nonlinear differential equation. Closed-form solution for this equation is impractical. For this reason, the response of the structure can be sought using numerical methods only.

Illustrative application

The formulation presented above is used in the following to evaluate the coupled galloping of a slender tower as an illustrative application. Figure 2 shows a positive train control tower consisting of a base tube and a swing tube, which are both rectangular Hollow Structural Steel sections. Table 1 lists the major dimensions of this tower.

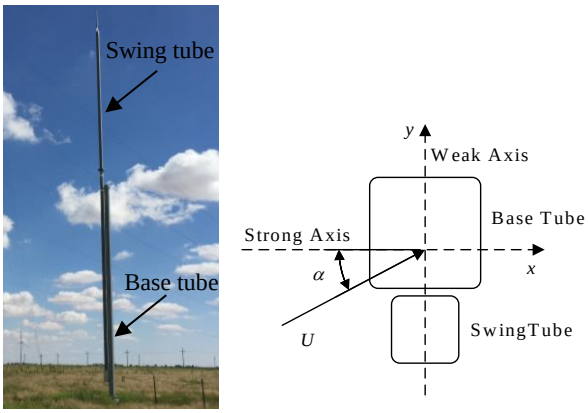

(a) (b)

Figure 2. (a) A positive train control tower and (b) coordinate system for description of wind and tower vibration

This tower was instrumented for monitoring because many failures of this type of tower due to wind-induced vibrations have been observed. The monitoring system consisted of accelerometers at three heights, one at the top of the swing tube, one at the top of the base tube, and one at a location that is 4.27

m from the lower end of the swing tube and three ultrasonic anemometers at heights of 2.44 m, 10 m and 18.5 m above ground level on an adjacent tower. All the sensors were continuously sampled at a frequency of 100 Hz. More details about the tower and the monitoring system can be found in a published previous study [3], which has identified the problematic vibrations to be coupled translational galloping. Figure 2 (b) shows the coordinate system that will be used subsequently to describe the measured wind speed and directions and vibrations of the tower.

	Width (cm)	Wall Thickness (cm)	Corner Radius/Width	Length (m)
Base Tube	21.0	0.74	0.07	9.3
Swing Tube	12.7	0.59	0.09	16.5

Table 1. Dimensions of the structural members of the tower instrumented for vibration measurements

In this study, numerical evaluation of the tower response based on the analytical formulation is achieved using the fourth-order Runge-Kutta method. This necessitates knowledge of the natural frequencies, damping ratios and shapes of the modes of interest, the force coefficients of the cross-sections of the tower, and the wind field in the boundary layer. The full-scale measurement data revealed that the large-amplitude vibrations are dominated by the fundamental modes about the weak and strong axes of the tower. For this reason, the numerical evaluation of the tower response will only consider these two modes, the frequencies of which are estimated to be 0.62 Hz and 0.7 Hz, respectively, based on the power spectral density functions of representative acceleration records. In a previous study [3], the damping ratios of these two modes were estimated using the logarithmic decrement method based on free vibration tests to be ζ_x=1.5% and ζ_y=1.4%, and the shapes of these two modes have been estimated through a finite-element model of the tower to be:

$$\begin{aligned}\phi_x(z) &= 7.777\times10^{-4}z^3 + 1.5399\times10^{-4}z^2 + 0.0241z \\ \phi_y(z) &= 1.102\times10^{-4}z^3 - 6.253\times10^{-4}z^2 + 0.0274z\end{aligned} \quad (17)$$

The force coefficients of the tower section consisting of the swing tube only and those of the section consisting of both the swing tube and the base tube have also been estimated in a previous study based on wind tunnel tests [3]. In this study, the force coefficients are approximated in the form of 7th order power series based on least squares fits. As an illustration, Figure 3 shows the drag and lift force coefficients of the swing tube (C_{D1} and C_{L1}) and those of the tower section consisting of the swing and base tubes (C_{D2} and C_{L2}) for a range of wind angle of incidence and the corresponding polynomial fits. It is assumed in this study that these force coefficients are not affected by the wind turbulence because the integral length scales of the wind over most of the height of the tower are much larger than the cross-sectional dimensions of the tower.

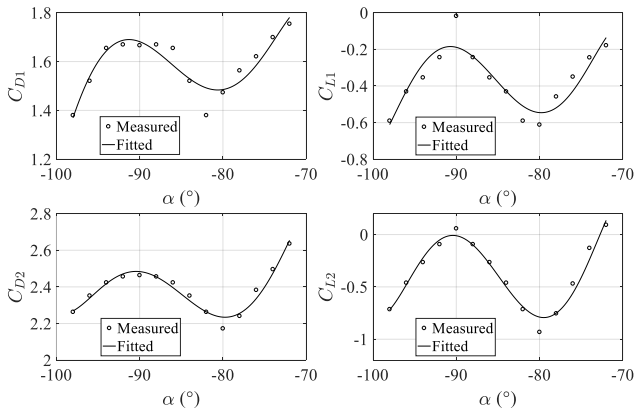

Figure 3. Force coefficients of the tower sections for -99°<α<-72°

To provide the excitation in the analytical model, the spectral representation method [16] is used to simulate the turbulence in the wind. The power spectral density functions of the turbulence are assumed to be of the Kaimal form, which can be expressed as

$$S_u(z,\omega) = \frac{200}{2\pi}u_*^2\frac{z}{\bar{U}(z)}\left[1+50\frac{\omega z}{2\pi\bar{U}(z)}\right]^{-5/3} \quad (18)$$

$$S_v(z,\omega) = \frac{15}{2\pi}u_*^2\frac{z}{\bar{U}(z)}\left[1+9.5\frac{\omega z}{2\pi\bar{U}(z)}\right]^{-5/3} \quad (19)$$

for the longitudinal and lateral components, respectively. In these expressions u_* is the friction velocity and ω is the circular frequency. The coherence function of the turbulence is assumed to follow that proposed by Davenport:

$$\gamma(\Delta z,\omega) = \exp\left[-\frac{\omega}{2\pi}\frac{C_z\Delta z}{\left[\bar{U}(z_1)+\bar{U}(z_2)\right]/2}\right] \quad (20)$$

where Δz is the distance between heights z_2 and z_1 and C_z is a constant. C_z=10 for longitudinal turbulence, and C_z=6.7 for lateral turbulence. The simulated turbulence field is superposed to a power-law mean wind speed profile to yield the complete wind field in the horizontal direction.

Figure 4 shows an example segment of wind speed and angle of incidence relative to the tower measured at the height of the top of the full-scale tower, and Figure 5 shows the displacements of the top of the tower as well as the instantaneous frequencies of the dominant modes of vibration, which were estimated by identifying the frequencies associated with the largest magnitude of the wavelet scalograms of the displacements at each time instant. Due to the variation of the mean wind speed and direction as shown in the graph, which are estimated through wavelet thresholding using a 11th order Daubechies 10 wavelet, the large-amplitude oscillations dominated by the component about the weak axes did not remain steady-state after the initial growth of the vibrtaion. However, it can be observed that when the vibration amplitudes were large, the vibration frequencies in the two orthogonal directions essentially coincide despite the fact that the natural frequencies of the modes in these two directions are considerably different. This suggests strong coupling between the vibrations in the two directions.

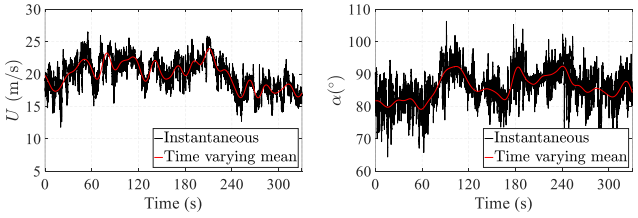

Figure 4. An example segment of wind speed and angle of incidence

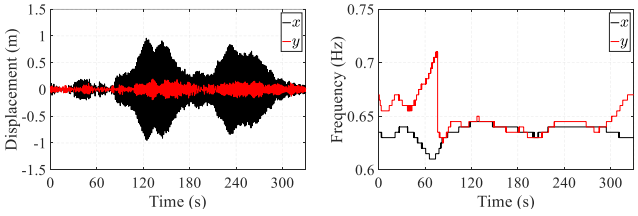

Figure 5. An example segment of displacement time histories and estimated instantaneous frequencies of the dominant modes

Figure 6 shows the time histories of the numerically simulated response of the tower at its top to the excitation of simulated wind field according to equations (18) to (20) that matches the mean wind speed and angle of incidence as well as the turbulence intensity of that presented in Figure 4. Also shown in this figure are the instantaneous frequencies of the vibrations. It can be seen

that the numerically simulated and measured vibrations reached similar amplitudes, and the coincidence of the frequencies due to coupling at large vibration amplitudes observed in the full-scale vibration can also be seen in the simulated vibrations.

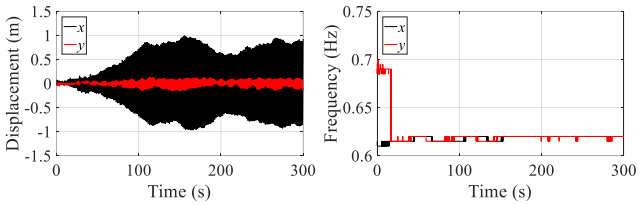

Figure 6. Numerically simulated displacement time histories and estimated instantaneous frequencies of coupled galloping oscillation

Because galloping instability of this tower occurs only over narrow ranges of wind angles of incidence [3], a comparison between the statistics of the recorded full-scale vibrations and simulated vibrations has not been achieved due to the challenges posed by the full-scale wind often being nonstationary. For this reason, only the dependence of the representative characteristics of the simulated vibrations on turbulence intensity are illustrated herein. Figure 7 shows the dependence of the RMS amplitude (σ_x and σ_y) and kurtosis (k_x and k_y) of the oscillation of the tower at its top at a mean wind speed of 20 m/s for a number of mean wind angles of incidence at which coupled galloping is determined to occur based on both full-scale data and numerical simulation. It can be seen that for this particular tower, the RMS amplitude of the dominant component of the vibration decreases with increasing turbulence intensity while the RMS amplitude of the other component is not significantly affected by the turbulence. It also can be observed that when the turbulence intensity is low, the vibration exhibits significant hardening non-Gaussian characteristics and that when the turbulence intensity becomes high, the vibration becomes closer to be Gaussian. This is significant for the performance of the tower as the distribution of the response critically affect the extreme and fatigue loading of the structure (e.g., [17]).

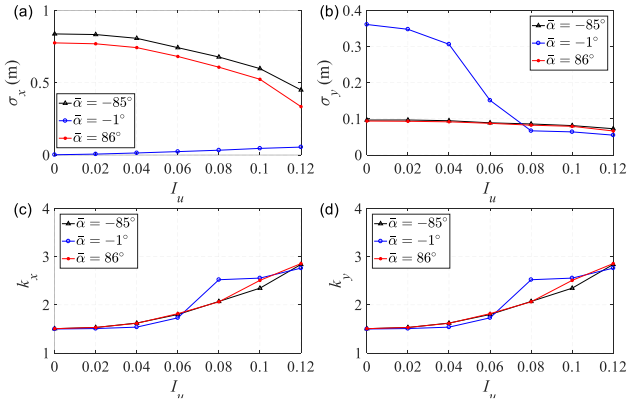

Figure 7 Dependence of the standard deviation and kurtosis of the vibration on turbulence intensity

Conclusions

An analytical model is developed based on the quasi-steady assumption to represent the nonlinearly coupled translational galloping of slender structures. This model is used as a basis to numerically evaluate the coupled galloping of a full-scale slender tower subjected to wind fields simulated using the spectral representation method. It is illustrated that the numerically simulated vibration can match the recorded full-scale vibration in characteristics in both amplitude and frequency. The results of the numerical evaluation also suggest that the turbulence intensity of the flow significantly affects the characteristics of the vibration that are critical for the extreme and fatigue loading of the structure. It is revealed that increasing turbulence intensity results in decreasing RMS amplitude of the dominant vibration component and that the response deviates more from the Gaussian distribution with decreasing turbulence intensity.

References

[1] Caracoglia, L., Influence of weather conditions and eccentric aerodynamic loading on the large amplitude aeroelastic vibration of highway tubular poles. *Engineering Structures*, 2007. 29(12): p. 3550-3566.

[2] Repetto, M.P. and G. Solari, Wind-induced fatigue collapse of real slender structures. *Engineering Structures*, 2010. 32(12): p. 3888-3898.

[3] Zuo, D., et al., Experimental and analytical study of galloping of a slender tower. *Engineering Structures*, 2017. 132: p. 44-60.

[4] Den Hartog, J.P., Transmission line vibration due to sleet. *transactions of the american institute of electrical engineers*, 1932. 51(4): p. 1074–1086.

[5] Novak, M., Galloping Oscillations of Prismatic Structures. *ASCE Journal of the Engineering Mechanics Division*, 1972. 98(EM1): p. 27-46.

[6] Parkinson, G.V., A tolerant wind tunnel for industrial aerodynamics. *Journal of Wind Engineering and Industrial Aerodynamics*, 1984. 16(2-3): p. 293-300.

[7] Novak, M. and H. Tanaka, Effect of Turbulence on Galloping Instability. *ASCE Journal of the Engineering Mechanics Division*, 1974. 100(EM1): p. 27-47.

[8] Richardson, A., Predicting Galloping Amplitudes. *Journal of Engineering Mechanics*, 1988. 114(4): p. 716-723.

[9] Jones, K.F., Coupled vertical and horizontal galloping. *Journal of Engineering Mechanics, ASCE*, 1992. 118(1): p. 92-107.

[10] Liang, S., et al., An evaluation of onset wind velocity for 2—D coupled galloping oscillations of tower buildings. *Journal of Wind Engineering and Industrial Aerodynamics*, 1993. 50(0): p. 329-339.

[11] Macdonald, J.H.G. and G.L. Larose, Two-degree-of-freedom inclined cable galloping--Part 1: General formulation and solution for perfectly tuned system. *Journal of Wind Engineering and Industrial Aerodynamics*, 2008. 96(3): p. 291-307.

[12] Macdonald, J.H.G. and G.L. Larose, Two-degree-of-freedom inclined cable galloping—Part 2: Analysis and prevention for arbitrary frequency ratio. *Journal of Wind Engineering and Industrial Aerodynamics*, 2008. 96(3): p. 308-326.

[13] Nikitas, N. and J. Macdonald, Misconceptions and Generalizations of the Den Hartog Galloping Criterion. *Journal of Engineering Mechanics*, 2014. 140(4): p. 04013005.

[14] Li, Q.S., J.Q. Fang, and A.P. Jeary, Evaluation of 2D coupled galloping oscillations of slender structures. *Computers & Structures*, 1998. 66(5): p. 513-523.

[15] Raeesi, A., S. Cheng, and D.S.K. Ting, A two-degree-of-freedom aeroelastic model for the vibration of dry cylindrical body along unsteady air flow and its application to aerodynamic response of dry inclined cables. *Journal of Wind Engineering and Industrial Aerodynamics*, 2014. 130: p. 108-124.

[16] Deodatis, G., Simulation of ergodic multivariate stochastic processes. *Journal of Engineering Mechanics*, 1996. 122(8): p. 778-787.

[17] Chen, X., Analysis of crosswind fatigue of wind-excited structures with nonlinear aerodynamic damping. *Engineering Structures*, 2014. 74(0): p. 145-156.